Electronic Supplementary Material (ESI) for Nanoscale.

Supplementary Material for "Manipulating crack path by surface functional groups of MXenes"

Yu Chen[1,4] Shengjie Tang[2] and Xin Yan[1,3]

[1] *School of Mechanical Engineering and Automation, Beihang University, Beijing, 100191 China*
[2] *Grote Industry, Madison, Indiana, 47250 USA*
[3] *Advanced Manufacturing Center, Ningbo Institute of Technology, Beihang University, Ningbo, 315100 China*
[4] *The 52nd Research Institute of China Electronics Technology Group Corporation, Hangzhou, 310000 China*

I. SUPPORTING FIGURES

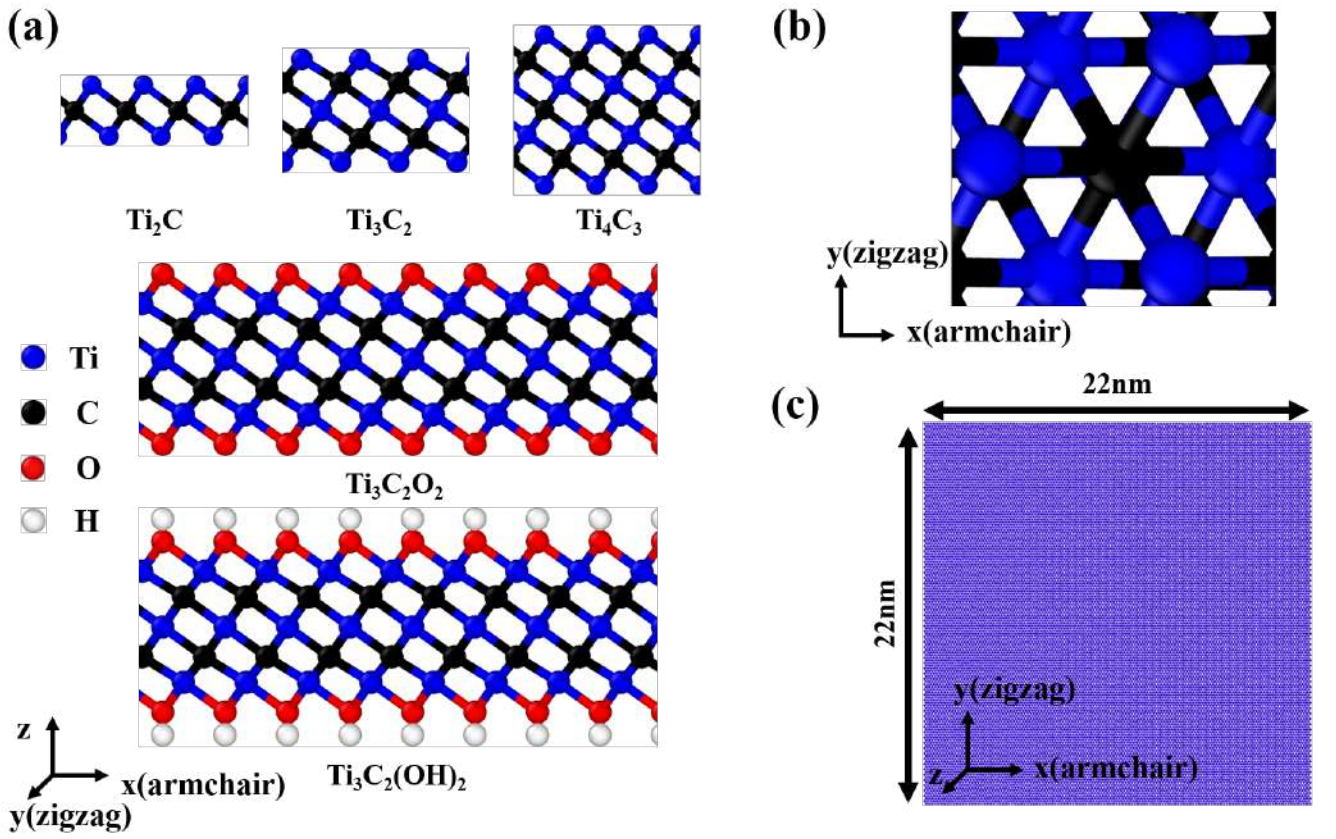

FIG. S1: Atomic structures of $T_{n+1}C_nT_x$. (a) The side view of $T_{n+1}C_n$, $Ti_3C_2O_2$ and $Ti_3C_2(OH)_2$. The blue, black, red and white atoms represented Ti, C, O and H atoms respectively. (b) Zoomed-in view of the in-plane atomic structure of Ti_3C_2. (c) The simulation model of tensile and shear testing simulation.

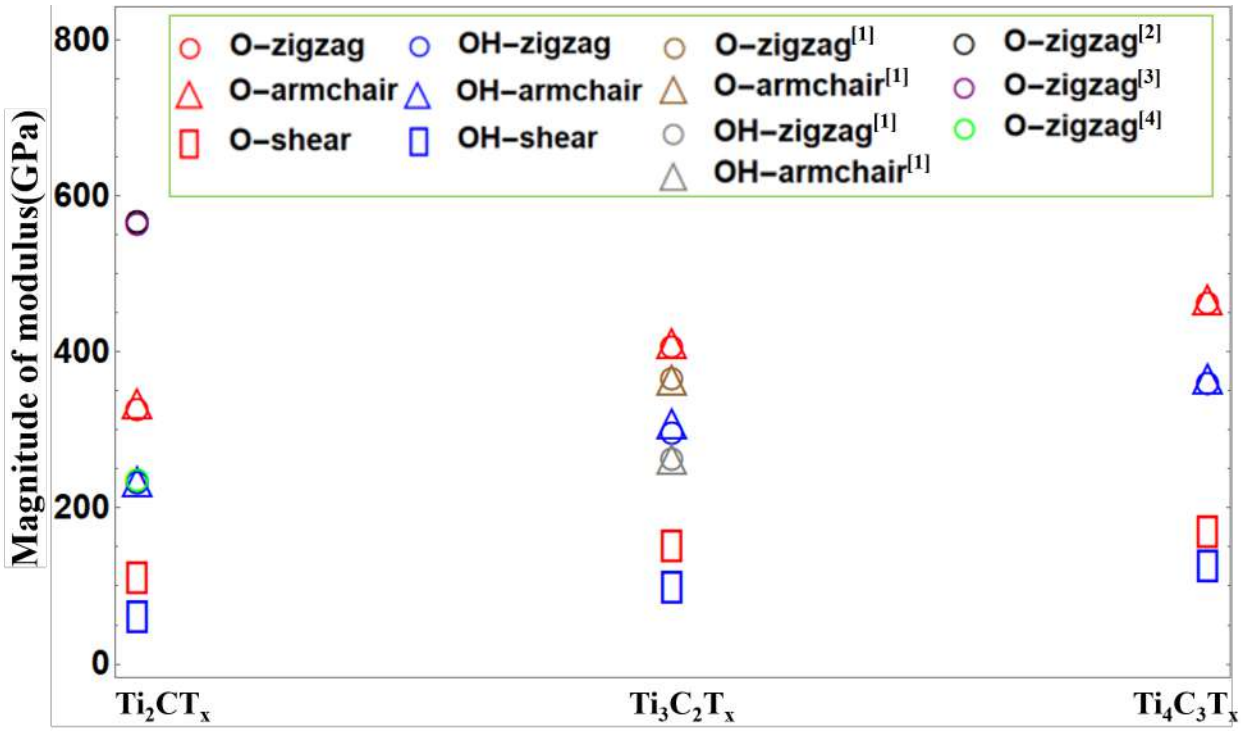

FIG. S2: The Young's modulus and shear modulus from our simulations. In order to explore the thickness effect on MXenes' mechanical property, we performed same tensile and shear simulation on Ti_2CT_x and $Ti_4C_3T_x$. This figure also include the results from other first principle calculations[1–4]. Based on the calculation, the thicker MXene would have higher modulus. It had been revealed that the thicker MXene would have a cohesive effect which would prevent fracture happening[5]. Besides, we could find that the magnitude of Young's modulus, shear modulus for the MXene with -O functional group was higher comparing with the one with -OH functional group.

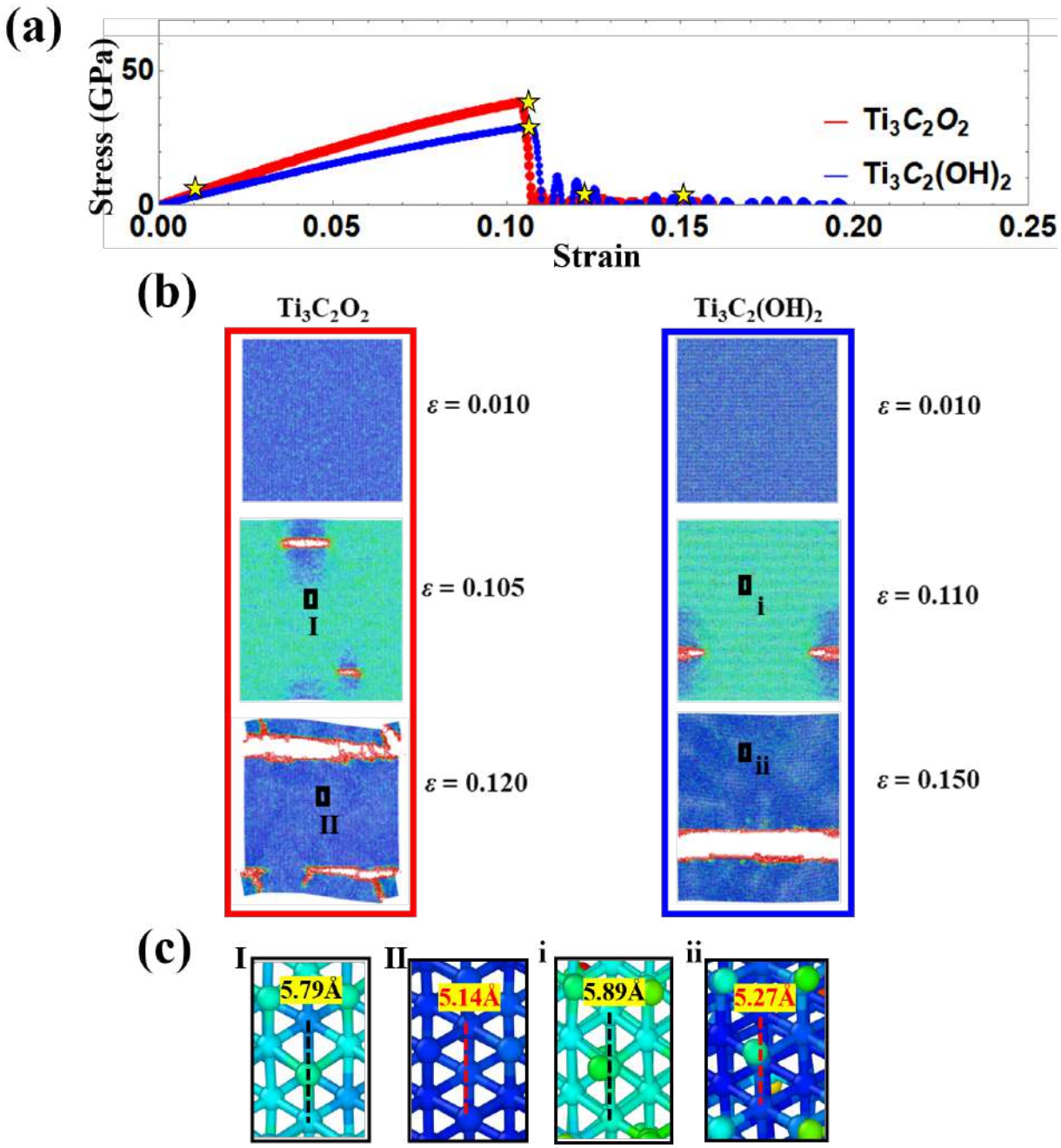

FIG. S3: The tensile simulation results of $Ti_3C_2T_x$ with detailed information (the curves were same as the ones Fig. 1c in the main text). (a) Stress-strain curves for stretching along the zigzag direction. The yellow stars indicated the strain stage of snapshots in b. (b) Snapshots of the atomic structure variation when stretching along the zigzag direction. The snapshots were colored by shear strain value and shared the same color bar shown in the upper right corner of the Fig. 1c in the main text. (c) Variation of the atomic structure during tensile loading. The snapshots labeled as I, II, i and ii were the zoomed-in view of the back-squared area in the second and third snapshots in the red and blue boxes in b.

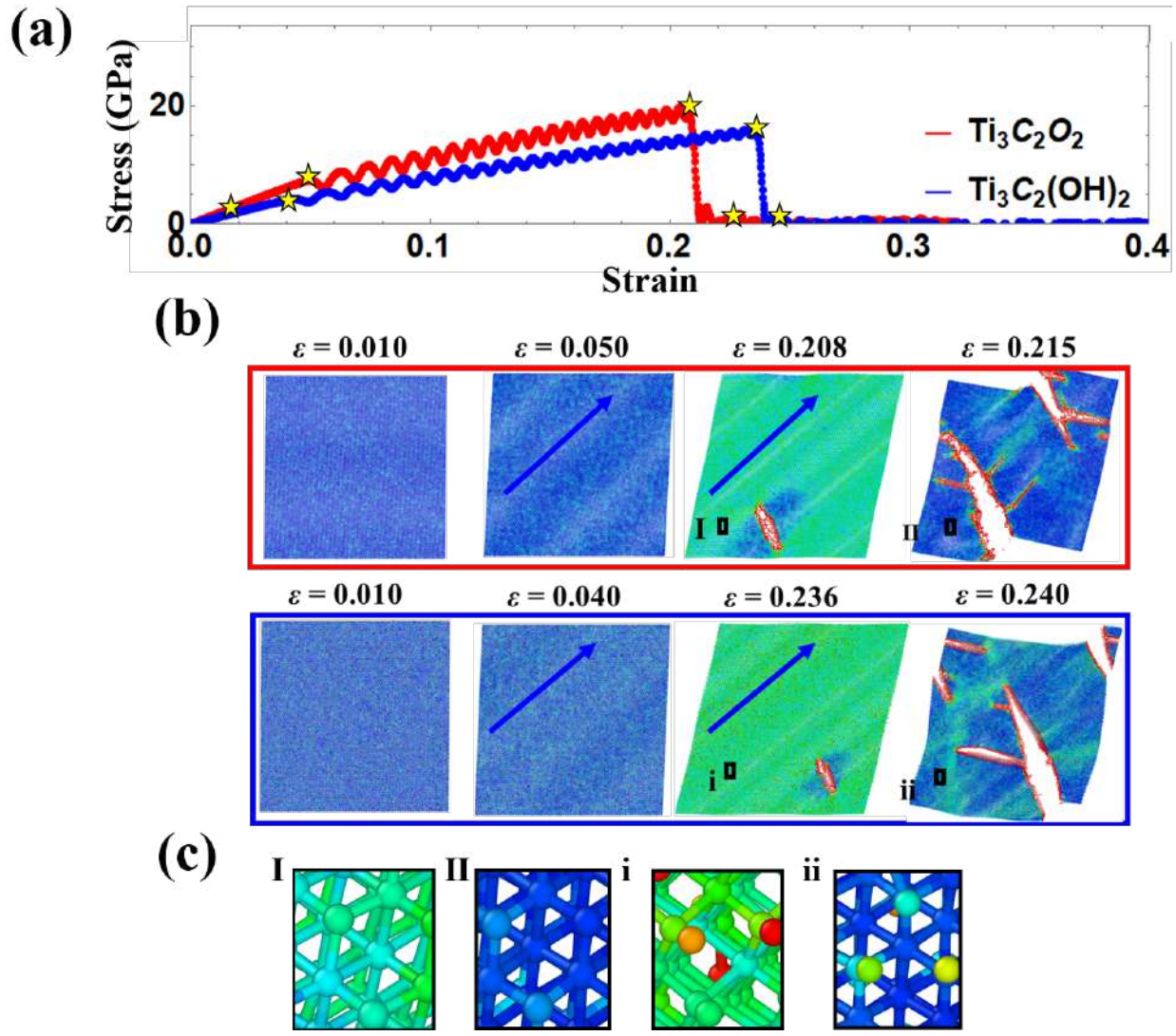

FIG. S4: The results of $Ti_3C_2T_x$ with detailed information under shearing (the curves were same as the ones in Fig. 1d in the main text). (a) Stress-strain curves of shear loading. The yellow stars indicated the strain stage of snapshots in b. (b) Snapshots of the atomic structure variation when shear loading was applied. The atoms were colored by shear strain value and shared the same color bar shown in the upper right corner of the Fig. 1c in the main text. (c) Variation of the atomic structure during shear loading. The snapshots labeled as I, II, i and ii were the zoomed-in view of the back-squared area in the third and fourth snapshots in the red and blue boxes in b.

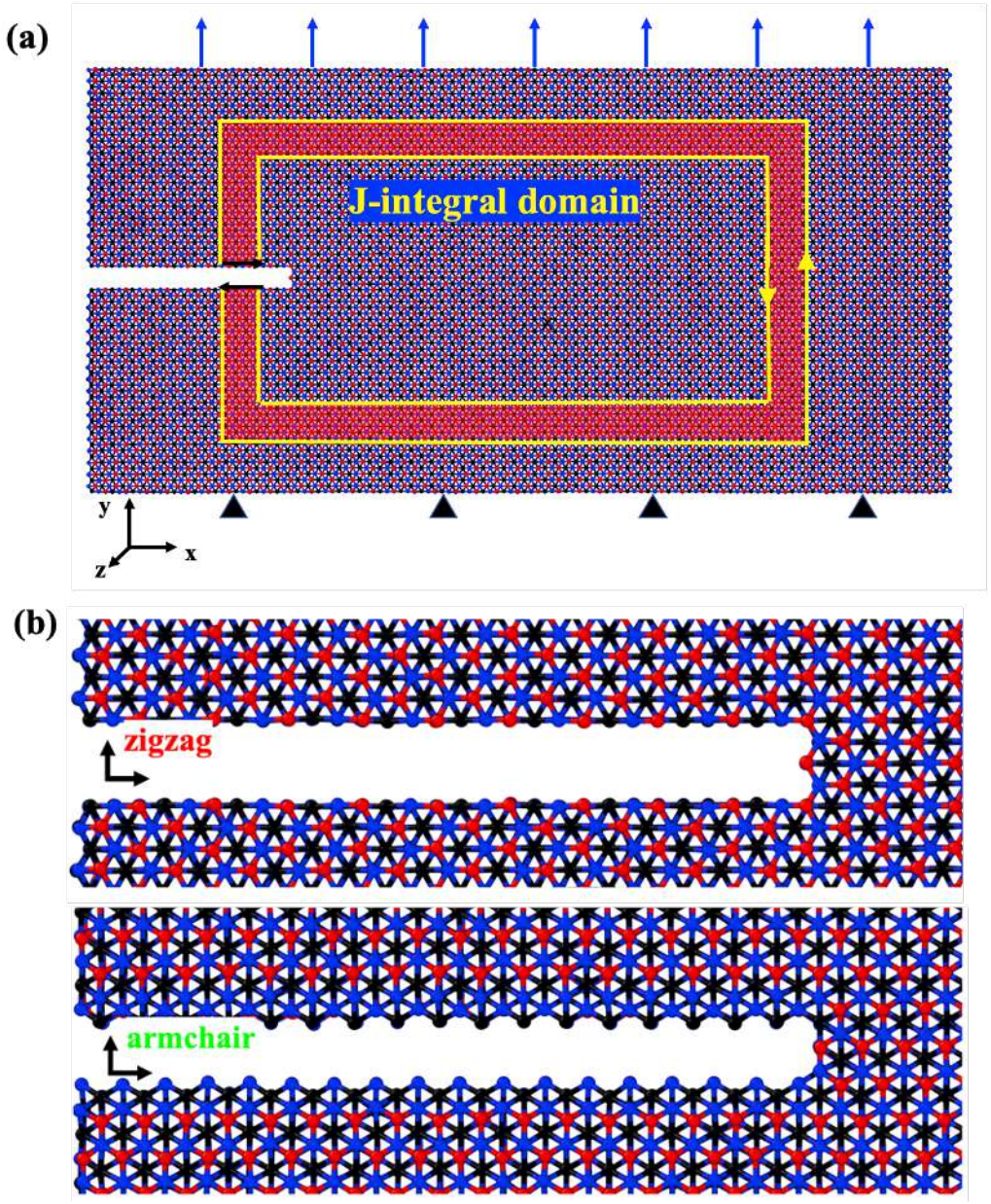

FIG. S5: (a)Model used for Mode-I crack testing of MXenes. The dimension of the model was approximately 22nm x 11nm in x and y directions. (b)Zoomed-in view of the initial crack for loading along zigzag and armchair directions. The size of the initial crack is 5nm x 0.6nm. The red area in a was for the calculation of J-integral and the J-integral calculation followed the method reported in a recent research[5].

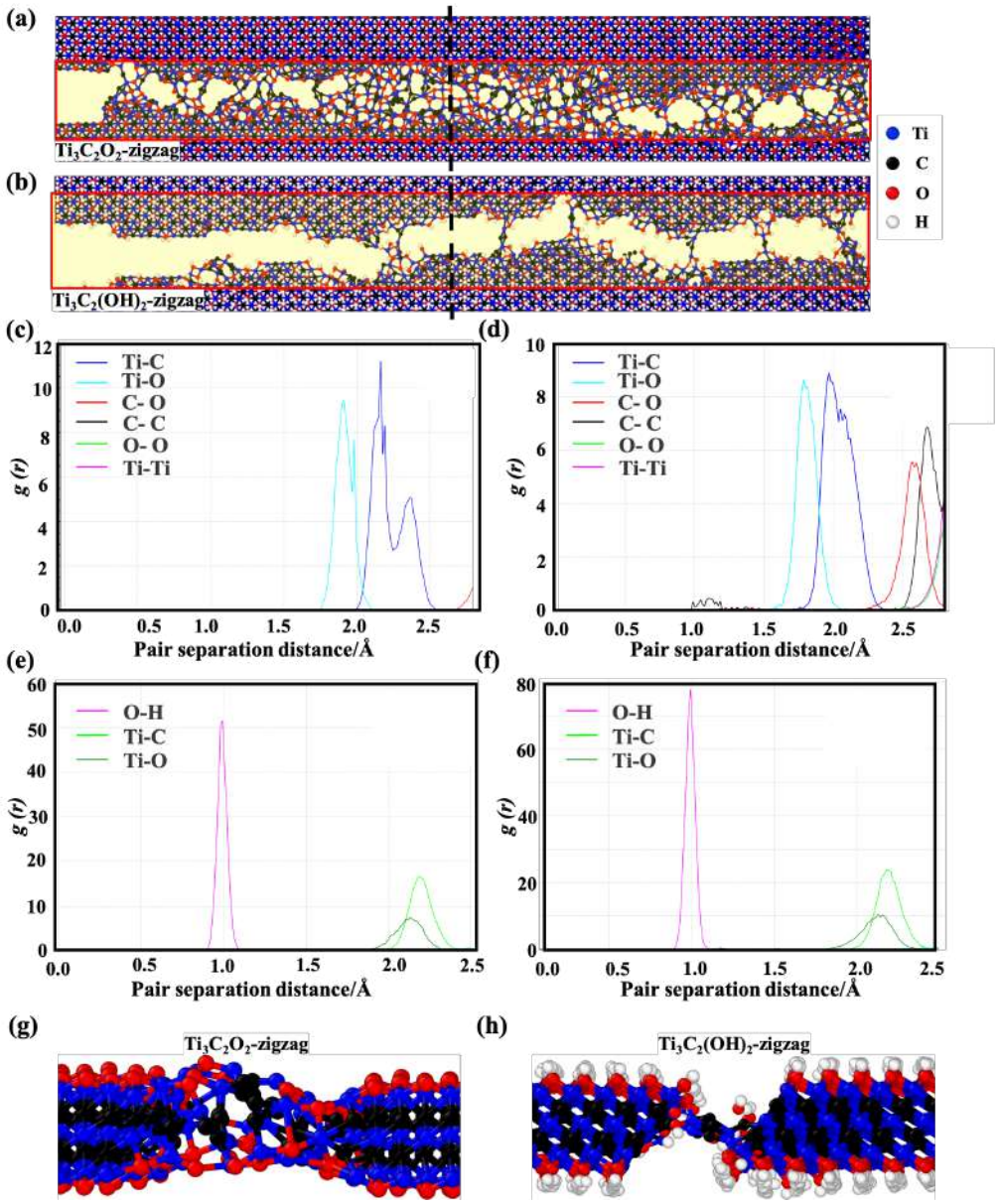

FIG. S6: The radial distribution function (RDF) for the $Ti_3C_2O_2$ and $Ti_3C_2(OH)_2$ loading along zigzag direction. (a)(b)The atoms in the red square were used for RDF calculation. (c)(d)RDF calculation results for the $Ti_3C_2O_2$ before and after crack propagation. (e)(f)RDF calculation results for the $Ti_3C_2(OH)_2$.(g)(h)Side view and structure schematic of middle cross-section (the black dashed line in Fig. S6a,b). When the crack propagated, the bonds connected the surface functional group (Ti-T bond) broke first. Then the middle layer Ti-C bond, and finally the Ti-C bond of the surface layer. Comparing between (c) and (d), we can find that new bonds of C-C and C-O appeared after crack propagation. Besides, we notice that the central position of Ti-O peak moves 0.084 Å(the yellow dashed lines indicate the position of the peak) left after the crack propagate through the sample which indicate some new Ti-O bonds appears. From (e) and (f), there is no new type of bonds appeared. Besides, the position of the peaks also at basically the same position before and after the crack propagation. Based on these observations, we could be able to draw the conclusion that for $Ti_3C_2O_2$, during the crack propagate through the sample, new C-C, C-O and Ti-O bonds appears and form the chains and network. While for $Ti_3C_2(OH)_2$, the bonds broken thoroughly without appearing new bonds which is main because of the dangling H stopping O working with other atoms. We can also find the new-formed network of $Ti_3C_2O_2$ sample from (g).

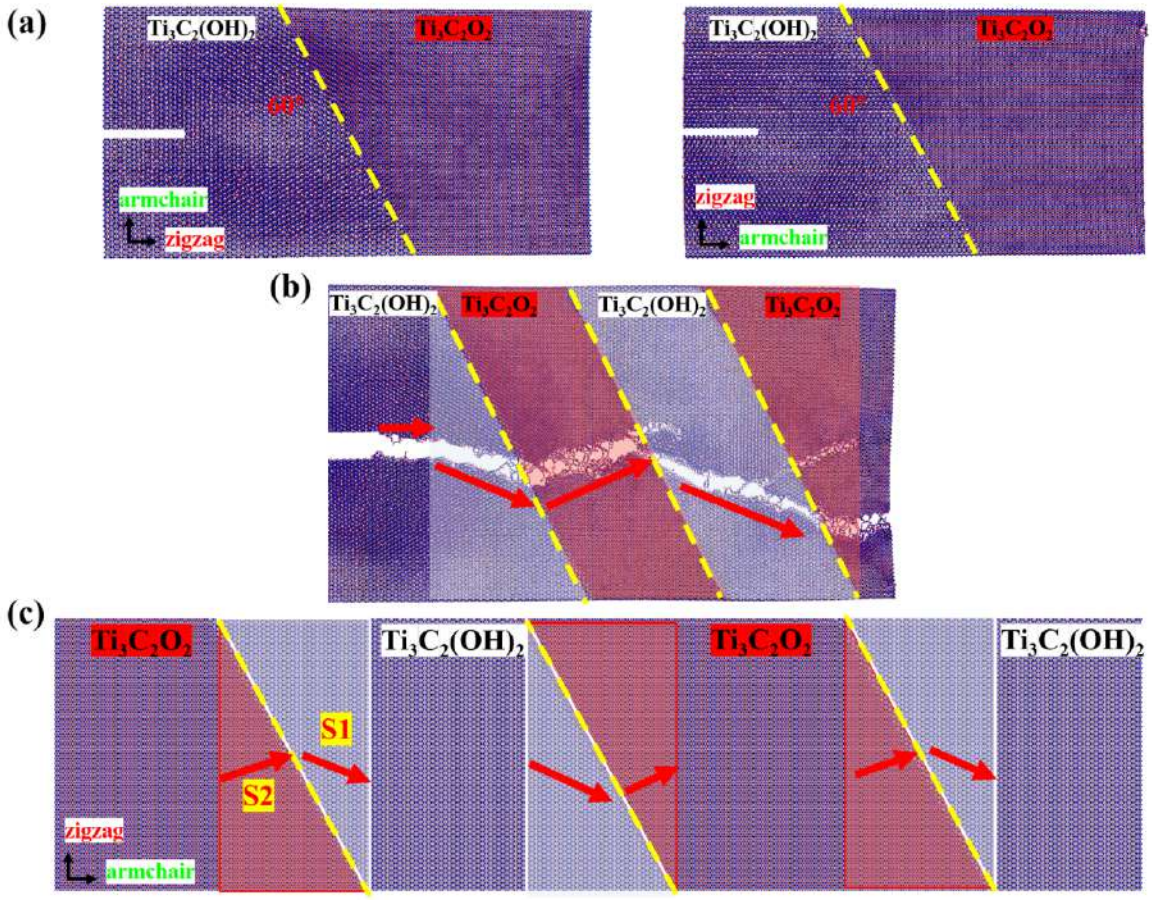

FIG. S7: Crack propagation through functional group interfaces (a) The crack expansion models which had functional groups interface, the yellow dashed lines indicated the interfaces. The angle between the interface and horizontal direction was 60°. The left and right models were for loading test along the armchair and zigzag directions, respectively. The left part of the interface was $Ti_3C_2(OH)_2$ in each model, and the right part was $Ti_3C_2O_2$. (b) The initial crack was in $Ti_3C_2(OH)_2$. The white shaded area represented $Ti_3C_2(OH)_2$ and the red shaded area represented $Ti_3C_2O_2$. (c) The crack expansion model which had a transition space between the interfaces, the red arrows represented the expected crack propagation directions.

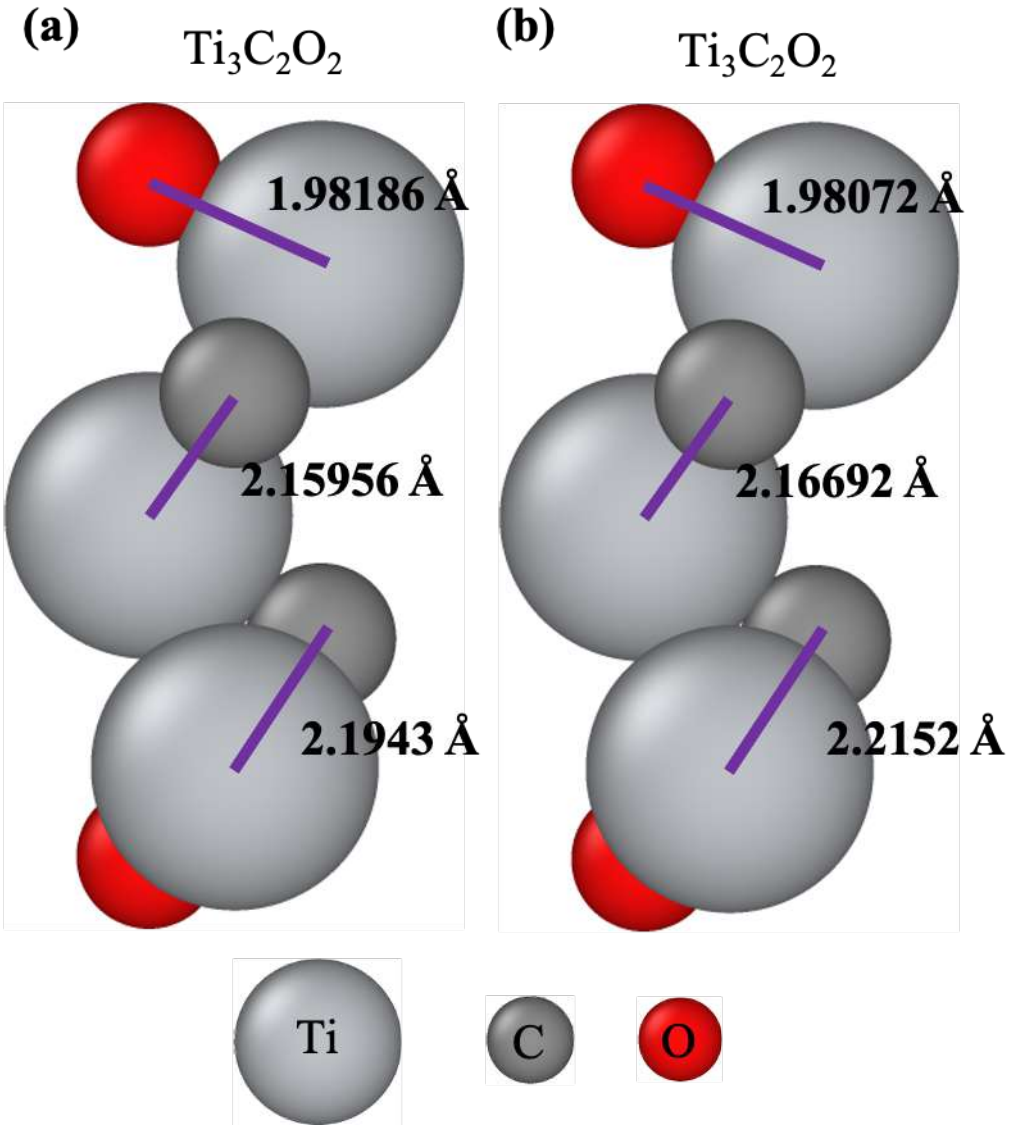

FIG. S8: Calculated bond distance (a) from Ref[6] and (b) in our simulation using reaxff potential[7].

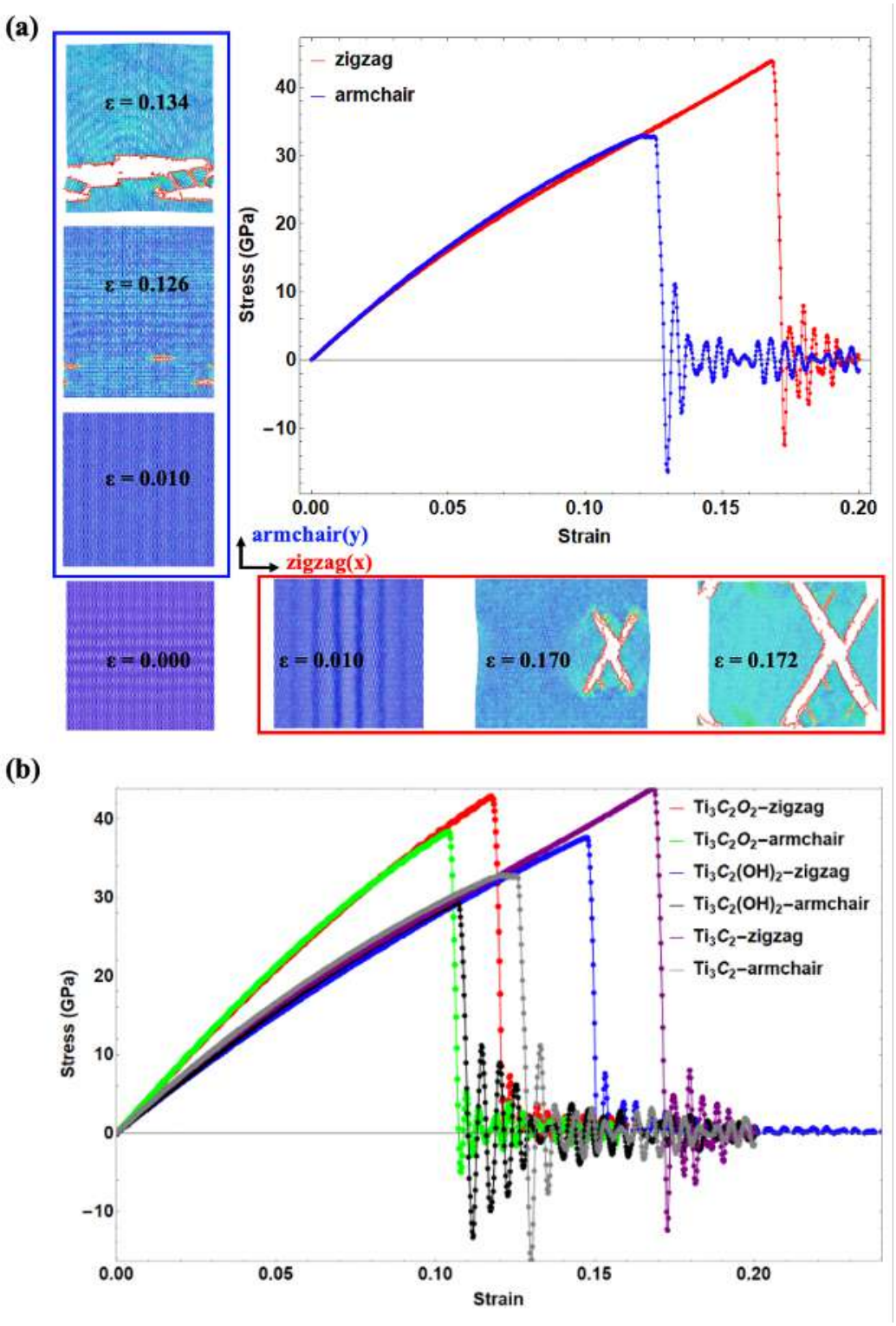

FIG. S9: (a)The simulation results of Ti_3C_2 loading from zigzag (red curve) and armchair (blue curve) directions. The snapshot in the left-bottom illustrates the initial structure. The snapshots in the blue box are corresponding to the blue curve and the snapshots in the red box are related to the red curve. The atoms are colored by shear strain value and shared the same color bar shown in the upper right corner of the Fig. 1c in the main text. For both loading cases, the crack initiate and propagate along the zigzag directions.(b)The stress-strain curves of the samples with and without functional groups are plotted together. Based on the comparison among the curves, we find that the -O functional group (red and green curves) affect the Young's modulus and the -OH functional group is mainly changing the strength of the sample (blue and purple curves).

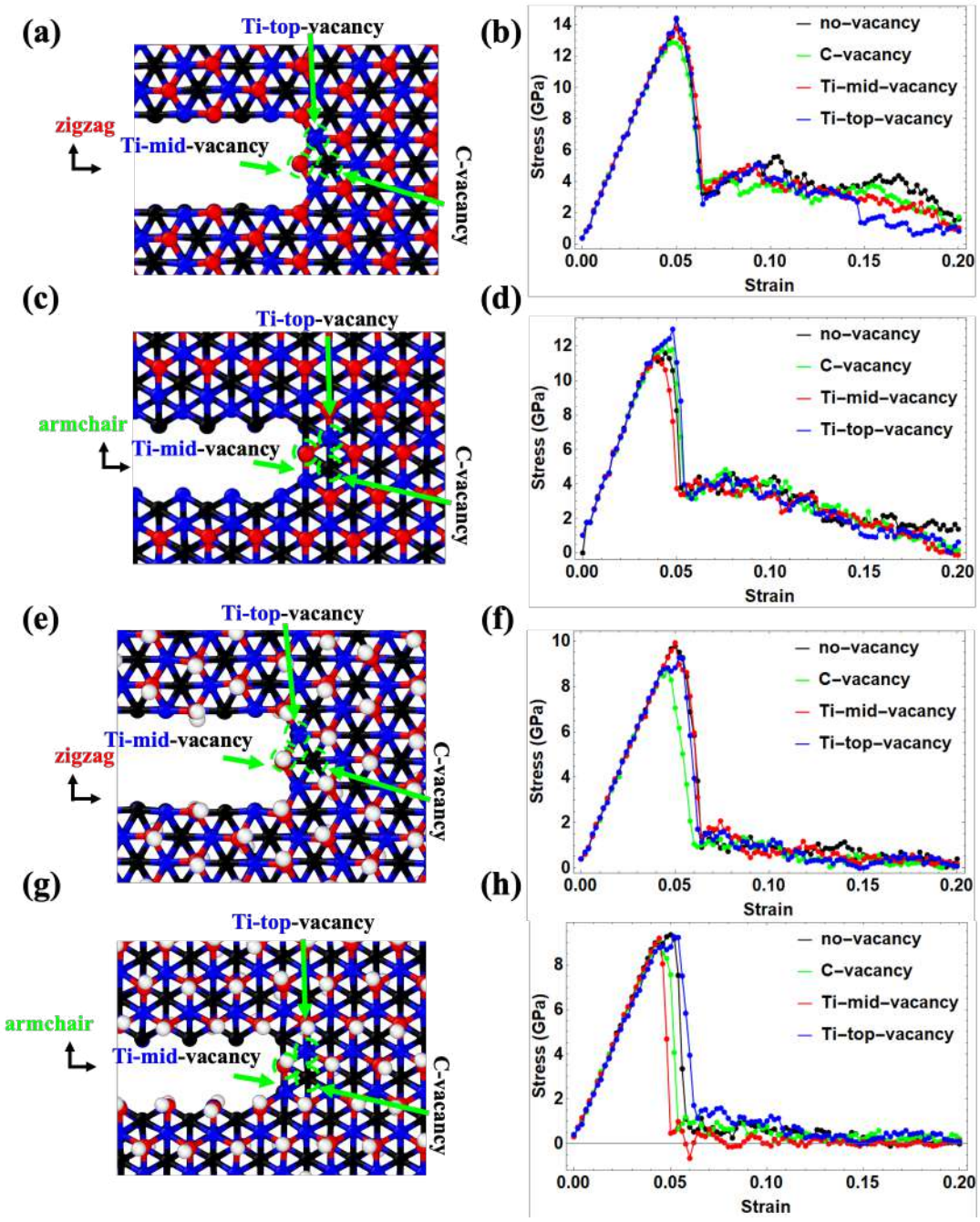

FIG. S10: The simulation of crack propagation of $Ti_3C_2(OH)_2$ and $Ti_3C_2O_2$ with different types of single atom vacancy ahead of the crack tip.Different type of vacancy ahead of the crack tip and corresponding stress-strain curves of (a)(b) $Ti_3C_2O_2$ loading along zigzag direction, (c)(d) $Ti_3C_2O_2$ loading along armchair direction, (e)(f) $Ti_3C_2(OH)_2$ loading along zigzag direction and (g)(h) $Ti_3C_2(OH)_2$ loading along armchair direction.

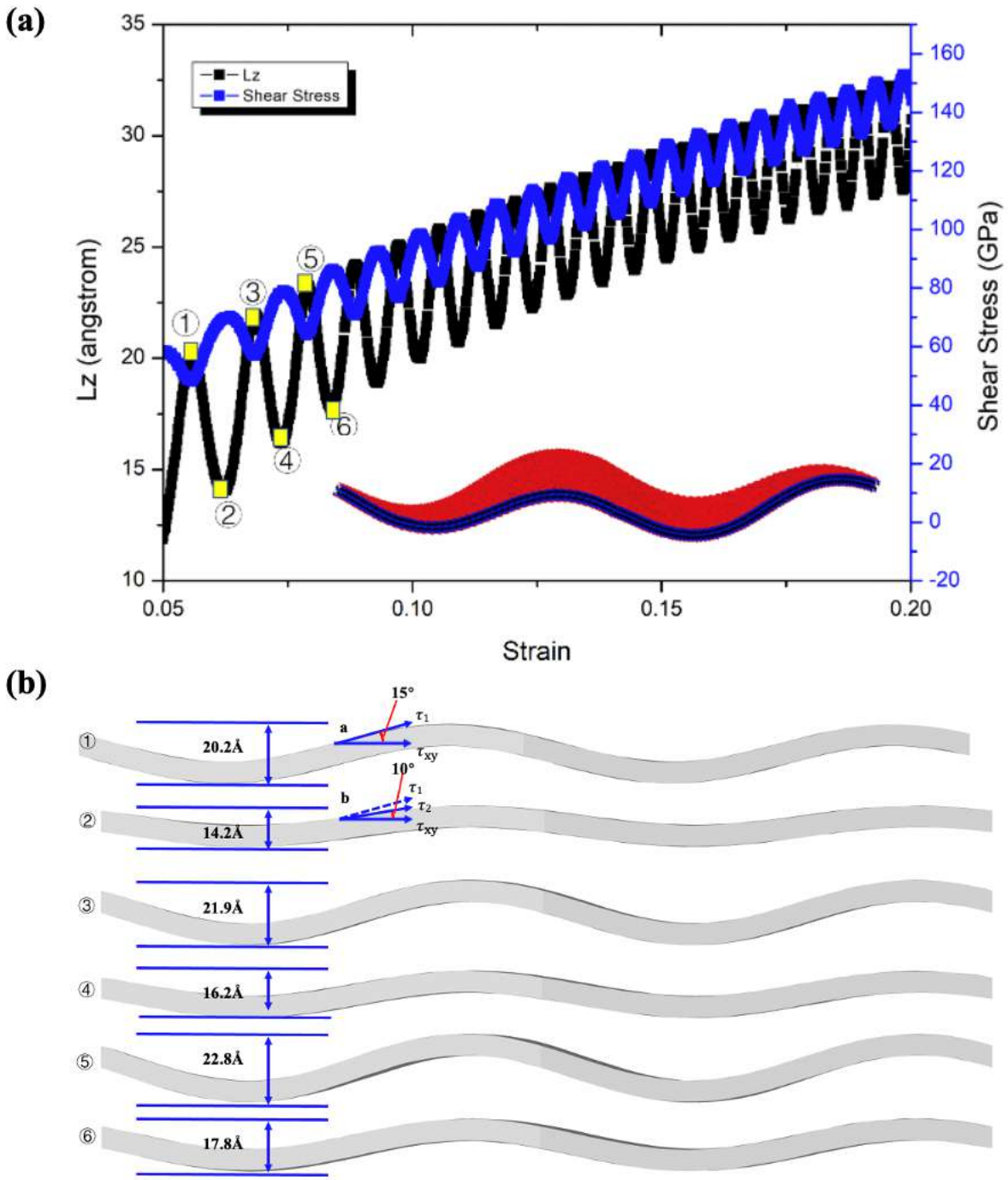

FIG. S11: (a)Part of stress-strain curve of shear loading of $Ti_3C_2O_2$;(b)buckling shape of $Ti_3C_2O_2$ at the specific points.

II. SUPPORTING NOTES:POTENTIAL VALIDATION

To verify the potential, We carried out a serious testing, including bonds distance, elastic constants, Young's module and rigidity coefficient, and compare our testing results with the first-principle calculations. For the bonds distance, we equilibrium the unit cell at 1 K and calculate the bond distance. Based on our calculation, the distance of Ti-O, Ti(top)-C and Ti-C(middle layer) are 1.98Å, 2.22Å and 2.17Å. The reported bond distance of compare the bond distance Ti-O, Ti(top)-C and C-O(middle layer) are 1.98Å, 2.20Å and 2.16Å in Ref.[6]. Please refer to Fig S8. We can tell all the bonds from MD simulation based on the reaxff potential (Fig. S8 b) are very close to the first principle calculation. About the elastic constant, we take the unit cell of $Ti_3C_2O_2$ and found C_{11}=591.8 GPa. In Ref.[8], the calculated C_{11} using first principle approach is 523 GPa. The Young's module of $Ti_3C_2O_2$ and $Ti_3C_2(OH)_2$(n=1,2,3)calculated in this work as well as other references are shown Fig. S2. Regarding bending rigidity, we adopted the methodology reported in [9] and found the bending rigidity for Ti_2C is 4.94 eV. The first principle calculated result is 4.47eV reported in Ref.[1] and the result from MD simulation using other potential (5.21eV)[9]. Based on these testing results, all these properties are consistent with first principle calculation from reported references. Thus, the potential we adopted in this work could capture the fundamental properties of $Ti_3C_2O_2$ and $Ti_3C_2(OH)_2$.

III. SUPPORTING NOTES:EXPLANATION OF SHEAR STRESS-STRAIN CURVES FLUCTUATION

During shear loading, the MXene buckled (Fig.S11 (a)) and the buckled shape changed cyclically (Fig.S11 (b)). This makes the thickness of the simulation box fluctuate as shown in the figure and in general there are two modes can be found. The shapes of the MXene membrane shown in figure b are corresponding to the points marked with numbers in figure a. Close scrutiny of figure a which is the plot of the simulation box thickness (Lz)and shear stress versus strain, we found that the fluctuation of the Lz is opposite to the fluctuation of shear stress. In our simulation, the shear stress we adopted is τ_{xy} as shown in the figure, and actual in plane shear stress is along the direction of τ_1. When the shape of the MXene change from 1 to 2. If take point a and b as an example, the in-plane stress varies from τ_1 to τ_2 and the corresponding angle between τ_{xy} and τ varies from to 15° to 10° roughly. From figure b, when the angle become smaller which means the thickness of the simulation box is smaller, the calculated shear stress in our simulation which is the projection of τ along y direction τ_{xy} become smaller, such as point 1, 3, 5, etc. When the thickness of the simulation box become smaller, the angle will become smaller and the projection will become bigger, which corresponds to the points of 2, 4, 6, etc. Thus, the cyclical fluctuation of stress value could be observed in our calculation.

[1] Z. Fu, Q. Zhang, D. Legut, C. Si, T. C. Germann, T. Lookman, S. Du, J. S. Francisco and R. Zhang, *Physical Review B*, 2016, **94**, 104103.
[2] P. Chakraborty, T. Das, D. Nafday, L. Boeri and T. Saha-Dasgupta, *Physical Review B*, 2017, **95**, 184106.
[3] Z. Guo, J. Zhou, C. Si and Z. Sun, *Physical Chemistry Chemical Physics*, 2015, **17**, 15348–15354.
[4] U. Yorulmaz, A. Özden, N. K. Perkgöz, F. Ay and C. Sevik, *Nanotechnology*, 2016, **27**, 335702.
[5] C. Wei and C. Wu, *Engineering Fracture Mechanics*, 2020, **230**, 106978.
[6] M. Khazaei, M. Arai, T. Sasaki, C.-Y. Chung, N. S. Venkataramanan, M. Estili, Y. Sakka and Y. Kawazoe, *Advanced Functional Materials*, 2013, **23**, 2185–2192.
[7] N. C. Osti, M. Naguib, A. Ostadhossein, Y. Xie, P. R. Kent, B. Dyatkin, G. Rother, W. T. Heller, A. C. Van Duin, Y. Gogotsi *et al.*, *ACS applied materials & interfaces*, 2016, **8**, 8859–8863.
[8] Y. Bai, K. Zhou, N. Srikanth, J. H. Pang, X. He and R. Wang, *RSC advances*, 2016, **6**, 35731–35739.
[9] V. N. Borysiuk, V. N. Mochalin and Y. Gogotsi, *Computational Materials Science*, 2018, **143**, 418–424.
[10] M. Ying, R. Zhao, X. Hu, Z. Zhang, W. Liu, J. Yu, X. Liu, X. Liu, H. Rong, C. Wu *et al.*, *Angewandte Chemie*, 2022, **134**, e202201323.
[11] Y. Lv, L. Min, F. Niu, X. Chen, B. Zhao, Y. Liu and K. Pan, *Nanocomposites*, 2022, **8**, 81–94.